JOURNAL OF MATERIALS SCIENCE 9 (1974) 1803–1808

Fracture strength of soda-lime glass after etching

E. K. PAVELCHEK, R. H. DOREMUS
Materials Division, Rensselaer Polytechnic Institute, Troy, New York, USA

The strength of soda-lime glass at liquid nitrogen temperature after various amounts of etching was measured. A median crack length of 6 μm was calculated from the results and a model of the etching process. It was found that the rate of etching at the crack tip was much lower than on the external surface. Measured distributions of strength for samples etched different depths were also in reasonable agreement with calculated distributions. The etching process itself was found to cause some weakening of the glass.

1. Introduction

Glass normally fails at low stresses, yet strengths up to 7×10^9 N m^{-2} (10^6 psi) are possible for soda-lime glass at liquid nitrogen temperatures [1]. Fracture proceeds from surfaces in tension, and originates at flaws or cracks in the glass [2]. The stress at the tips of these cracks is much higher than the applied stress, and leads to low fracture stress. From a solution of the elastic equations Inglis [3] deduced the following relation between stress σ at the tip of an elliptical crack and the tensile stress S applied normal to the crack:

$$\sigma = S\left(1 + 2\sqrt{\frac{L}{\rho}}\right) \qquad (1)$$

where L is the length of the crack and ρ is the radius of curvature of the crack tip.

Direct measurements of dimensions of crack tips are not available. In most practical cases cracks in glass are submicroscopic in width. If it is assumed that the radius ρ of crack tips in a particular glass is constant, then from Equation 1 the fracture stress S_f to reach the ultimate stress σ_t at the crack tip should be inversely proportional to the square root of the crack length when $\sigma_t \gg S_f$. Such a dependence has been found by Griffith [2] and Mould and Southwick [4]. Mould and Southwick measured the fracture stress at liquid nitrogen temperature, thus avoiding time-dependent effects. They found cracks with lengths from 5 to 23 μm long in microscopic slides of soda-lime glass.

More information about cracks in glass can be derived from experiments on etching the glass surface. Proctor measured the fracture stress of glasses etched various amounts with hydrofluoric acid [5]. However, the amounts etched off were much greater (20 to 2000 μm) than the lengths of the cracks expected to be present in the glass, and the tests were carried out under ambient conditions and were, therefore, subject to static fatigue. Thus it is difficult to draw conclusions about crack geometry from Proctor's results.

In this work we slightly etched glass samples, and measured their strength at liquid nitrogen temperatures to avoid static fatigue. From the results we conclude that the tips of the cracks were etched only a small amount, and so were relatively inaccessible to the etching solution. It was possible to estimate the length of the cracks in the glass from the strength at different etch depths and at liquid nitrogen temperature. Various models for the etching process are discussed and compared with the experimental data.

2. Experimental

The test material was a commercial soda-lime glass, Kimble R-6, of approximate composition 68 wt % SiO_2, 15% Na_2O, 5% CaO, 4% MgO, 3% Al_2O_3, 2% BaO, 1% B_2O_3, and lesser amounts of other oxides. Rods of nominally 3 mm diameter were inspected for uniformity of diameter ($\pm \frac{1}{2}$%) using a micrometer, and cut into twenty 5 cm lengths. These rods were abraded by rotating in contact with fresh 400-grit SiC paper. The majority of the specimens were etched one-by-one in unstirred 1 to 10%

hydrofluoric acid, washed in tap water, rinsed in distilled water, and dried in air.

The amount of etching was determined by weighing the individual rods before etching, then reweighing after drying. In the earliest experiments (and lighter etches) each rod was weighed; later every third rod was weighed. The weighing was to within ± 0.000 01 g on a Mettler balance. The amount lost by abrasion was typically 0.000 02 g, and was considered insignificant, since the amounts etched ranged from 0.0002 to 0.012 g. The amount etched was calculated from the weight loss, density and computed surface area.

A second series of samples was etched as groups in a special holder that separated them. The solution, ½% HF and ½% H_2SO_4, was stirred. A third set of samples was immersed in water for 24 h after individual etching, and then dried in air 24 h before testing.

Care was taken not to touch the central sections of the rods after etching. The samples etched in a stirred solution and a majority of the others were allowed to stand in air for approximately 2 h, then tested to breaking while immersed in liquid nitrogen. The load was measured by an Instron tensile machine and applied through a four-point bending jig with an inner span of 1.25 cm.

Standards were made by following the same procedure as above, including rinsing, but excluding etching and weighing. The first sets evidenced some trouble in inserting the rods without touching the bending jig. A larger jig was used in subsequent tests, with no apparent change in results.

Sight checks for wetting angle were carried out by touching a water drop to freshly fractured, fire-polished, furnace-heated and aged surfaces. No high contact angles were observed, although the contact angle on fire-polished surfaces could be observed to decrease during a few seconds. A brief check of the etching rate of a fire-polished rod was made by placing it in 10% HF for 10 sec. The weight loss for fibre-polished rods was 2.71×10^{-3} g $\pm 0.38 \times 10^{-3}$; the abraded rods lost $3.01 \pm 0.16 \times 10^{-3}$ g.

3. Results

Table I shows the average breaking strength, the 95% confidence limit, and the ratio S/S_0 of average strengths after etching, to average strengths before etching. The Table also gives S/S_0 for median strengths, where the median value is the one with equal numbers of stronger

TABLE I Breaking strengths of soda-lime glass at −196°C after etching

Etch depth (μm)	Average breaking strength S		95% Confidence limits (%)	S/S_0 (average)	S/S_0 (median)
	$N\,m^{-2} \times 10^7$	psi × 10^3			
Samples etched individually					
0	12.7	18.5	± 4.3	1.00	1.00
0.18	15.6	22.7	5.2	1.22	1.22
0.53	14.0	20.3	7.5	1.09	1.12
1.28	17.6	25.5	5.3	1.38	1.28
2.73	20.9	30.3	14.9	1.64	1.51
5.08	38.1	55.3	23.2	2.98	2.08
6.40	87.5	127.0	24.1	6.85	5.93
9.42	97.0	140.8	44.3	7.60	3.30
9.60	61.5	89.2	34.3	4.81	4.40
Samples etched in groups					
0.63	15.3	22.2	6.9	1.20	1.29
1.13	13.7	19.8	11.8	1.07	1.02
2.00	31.0	45.0	21.3	2.43	2.09
2.67	25.2	36.5	24.4	1.72	1.56
Samples etched individually, then aged 24 h in water and 24 h in air before testing					
0	16.6	24.1	2.2	1.00	1.00
0.3	16.2	23.5	8.9	0.98	1.06
0.6	16.5	24.0	7.7	0.99	1.10
4.1	38.4	55.8	25.6	2.31	2.14

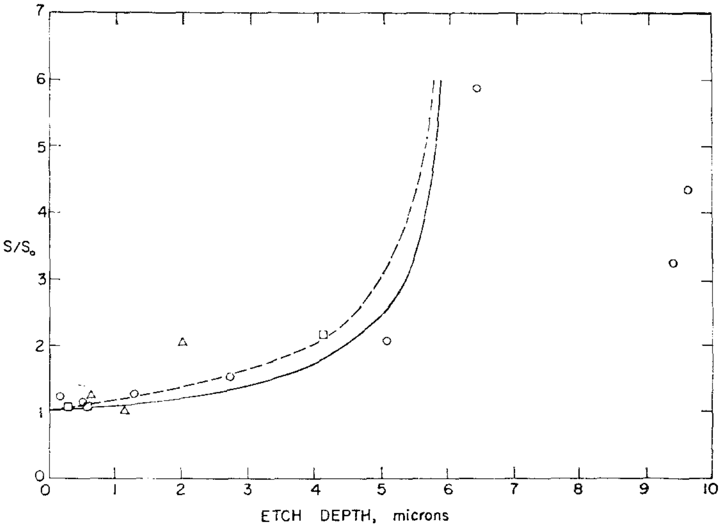

Figure 1 Relative median fracture stresses of rods of soda-lime glass at −196°C as a function of etching depth. ○, etched individually; △, etched in groups; □, etched individually and then aged 24 h in water and 24 h in air before testing (see Table I). Solid line from Equation 2 with $L_0 = 6 \mu m$; dashed line from Equation 4 with the same L_0 and ρ_0, and $\alpha = 2 \times 10^{-4}$, and $\rho_0 = 2 \times 10^{-7}$ cm.

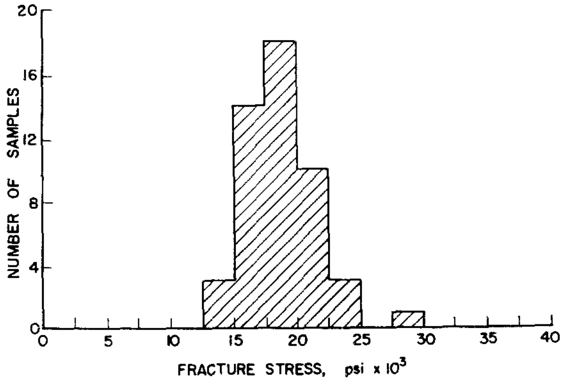

Figure 2 Distribution of strength at −196°C of unetched soda-lime glass.

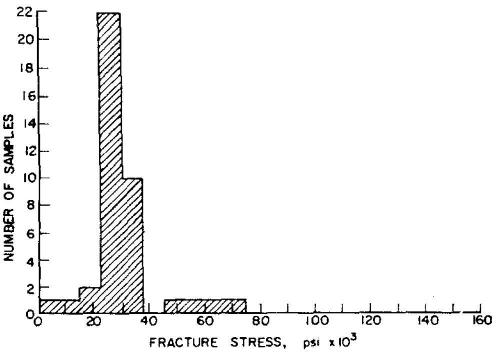

Figure 3 Distribution of strength at −196°C of soda-lime glass etched 2.73 μm.

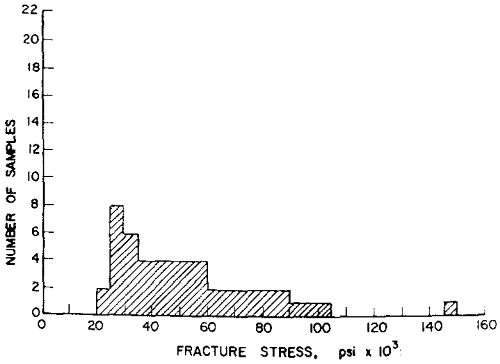

Figure 4 Distribution of strength at −196°C of soda-lime glass etched 5.08 μm.

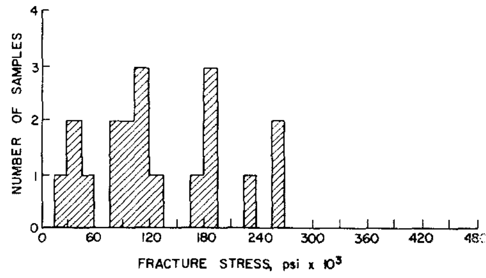

Figure 5 Distribution of strength at −196°C of soda-lime glass etched 6.4 μm.

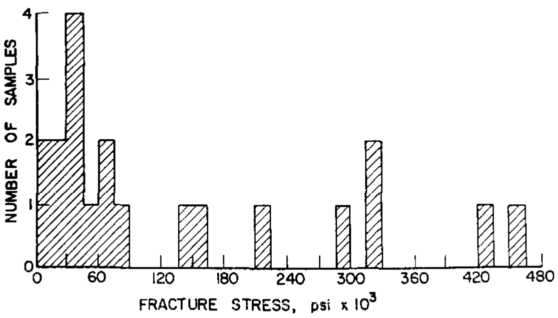

Figure 6 Distribution of strength at -196° C of soda-lime glass etched 9.4 μm.

and weaker samples. The median is considered to be more significant for comparison with various models of etching, because the distribution functions for larger amounts of etching are highly skewed. The average for a skewed distribution is distorted, and values for high strengths are uncertain, as mentioned below.

Samples aged in water for 24 h after etching were about 30% stronger than unaged samples, but the change in strength with etch depth was about the same as for unaged samples.

The larger errors for samples etched more than 6 μm are probably related to chemical effects during etching and greater sensitivity of etched surfaces to accidental damage, as discussed below.

The ratios of the median strengths after etching to the unetched strength are shown in Fig. 1 for all the data of Table I. Distribution of strengths for unetched and etched rods are shown in Figs. 2 to 6. The distribution becomes more skewed as etching proceeds. Noteworthy are the maximum strength of about 3.17×10^9 N m^{-2} (460 000 psi) and the large number of samples etched to 9.4 μm that are quite weak.

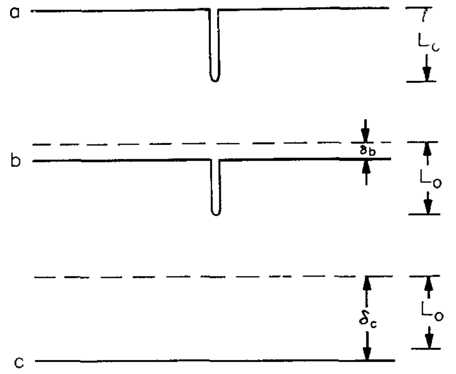

Figure 7 Model I. Etching of crack with no penetration of etchant into crack. L_0, initial crack length; δ, etch thickness.

4. Discussion

In this section various models for the etching process are presented and compared with the experimental data. Two extreme models of the etching process can be imagined [5]. In the first, illustrated in Fig. 7, no etching occurs in the crack, the tip radius remains constant, and the sample grows stronger as the crack becomes shorter.

From Equation 1 the fracture stress S needed to propagate a crack of length L and tip radius ρ is,

$$S \approx \frac{\sigma_t}{2} \sqrt{\rho/L}$$

since $L \gg \rho$. σ_t is the cohesive strength of the material. The etch depth δ equals L_0–L, where the subscript $_0$ indicates the unetched condition. For model I, ρ and σ_t are constant, so

$$\frac{S}{S_0} = \sqrt{\left(\frac{L_0}{L_0 - \delta}\right)} \cdot \tag{2}$$

In the second model, shown in Fig. 8, the length of the crack remains nearly constant, and the tip radius $\rho = \rho_0 + \delta$. Then

$$\frac{S}{S_0} = \sqrt{\left(1 + \frac{\delta}{\rho_0}\right)} \cdot \tag{3}$$

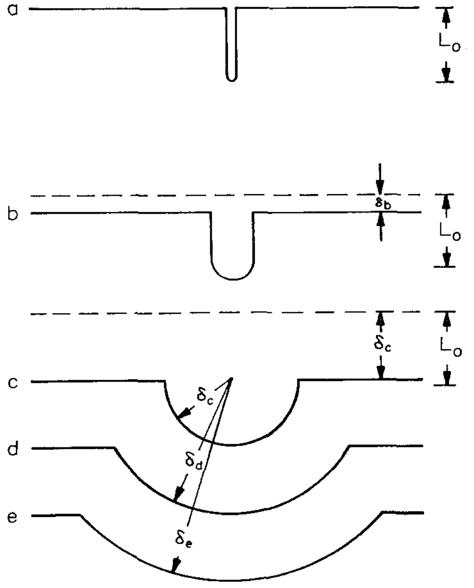

Figure 8 Model II. Etching of crack with etchant penetration and rounding of tip. L_0, initial crack length; δ, etch thickness.

Since ρ_0 is very small (about 20 Å, see calculation below), the strength should increase very sharply with etch depth according to Equation 3. The data in Fig. 1 do not show this sharp increase, therefore we conclude that little etching occurs at the crack tip.

From the distribution of strengths of unetched rods (Fig. 2) one can conclude that there is a distribution of values of the ratios of tip radii to crack lengths, ρ/L, for different flaws in the sample. If the distribution was entirely in ρ (all flaw lengths the same), there would not be a skewed distribution of the type shown in Figs. 4 to 6 after appreciable etching. Thus it seems that there is at least some distribution in flaw length.

The median strength as a function of etching depth, up to an etch depth of the initial median length, can be calculated directly from Equation 2, even if there is a distribution of flaw lengths. The results of such a calculation, assuming an initial median flaw length of 6 μm, are compared with the experimental data in Fig. 1. The calculated curve compares fairly well with the experimental one up to an etching depth near the initial crack length of 6 μm. Curves for lower (5 μm) or higher (7 μm) initial crack lengths show poorer agreement with the experimental data.

The theoretical strength of the glass is about 1.4×10^{10} N m^{-2} (2×10^6 psi). This result comes from a calculation of density of Si–O bonds with an energy of about 106 kcal mol^{-1} [6]. This strength should be reliable within limits of about ± 25%; the maximum strength measured for a high-alkali glass is about 10^{10} N m^{-2} (1.4×10^6 psi). With this theoretical strength, a fracture strength of 1.27×10^8 N m^{-2} (18.5×10^3 psi), and a crack length of 6 μm, the tip radius ρ is calculated to be about 20 Å from Equation 1.

Any calculated curve for model I (no etching of the tip) for an initial crack length of about 5 μm or longer falls somewhat below the data at shorter etch depths, as shown in Fig. 1 for $L_0 = 6$ μm. One reason for this discrepancy could be a small but appreciable etch rate of the tip. If the etching rate at the tip relative to that at the surface is α, Equation 3 can be written:

$$\frac{S}{S_0} = \sqrt{\left(1 + \frac{\delta\alpha}{\rho_0}\right)}\,.$$

The complete dependence of fracture stress on etch depth is then

$$\frac{S}{S_0} = \sqrt{\left[\left(\frac{L_0}{L_0 - \delta}\right)\left(1 + \frac{\delta\alpha}{\rho_0}\right)\right]}\,. \qquad (4)$$

The dotted curve in Fig. 1 was calculated from Equation 4 with the assumption that α was constant with etch depth and equal to 2×10^{-4}. In the calculation ρ_0 was taken to be 20 Å and L_0 6 μm; the calculated curve fits the experimental data better than the curve with $\alpha = 0$. It is possible that α is a function of crack depth, but the experimental data are not accurate enough to determine this functional dependence with any certainty.

The most likely reason for the low etching rate at the crack tips is that the etching solution in the cracks becomes rapidly saturated with reaction products, which diffuse out of the cracks only slowly because they are so narrow. The solubility of sodium fluorsilicate (Na_2SiF_6) is 6.5×10^{-3} g cm^{-3} at 17°C, or 6.9×10^{-5} mol of sodium ions per cm^3, so that the sodium ions in the glass, with a concentration of 1.2×10^{-2} moles per cm^{-3}, can saturate the solution after only a small amount of etching. If this saturation is the cause of low α values, then α should not change much except near the glass surface, as assumed in the last paragraph.

The highest strength found for etched glass in this study was 3.2×10^9 N m^{-2} (4.6×10^5 psi), and many samples of etched glass had lower strengths, even after the flaws were supposed to be completely etched away. Proctor found similar results, even with much deeper etching [5]. The reason why many etched samples have lower strengths is not certain. Great care was used in handling the samples before testing them, but accidental mechanical damage is always a possibility. It also seems likely that the etching process itself may introduce additional surface flaws by chemical processes. The details of such introductions are unclear.

After etching, the surface of the glass used in this study and many others [7, 8] appears pitted and uneven. These etch marks remain after etching much deeper than 6 μm. Thus it appears that the etch rate in the crack near the glass surface is not much different from the rate on the flat surface. A possible model III where some etching occurs in the crack but none at the tip, is shown in Fig. 9. This model gives rise to depressions in the surface of even heavily etched glass, which can increase the stress at their base up to a factor of three for a hemisphere. Thus the highest strength obtainable by this model of

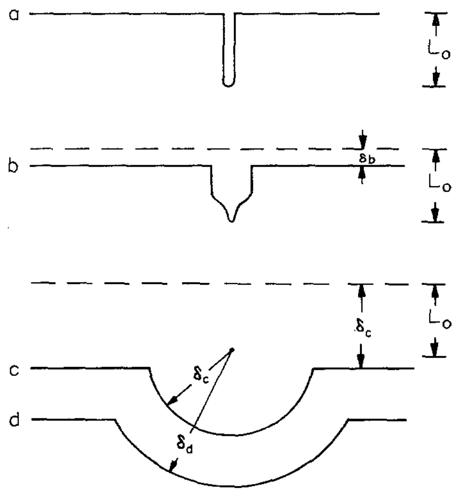

Figure 9 Model III. Etching of crack with partial penetration of etchant into the crack, but no tip rounding. L_0, initial crack length; δ, etch thickness.

etching would be about $\frac{1}{2}$ to $\frac{1}{3}$ of the theoretical strength. The maximum strength of etched glass found in this study was not too much below this limit.

In the discussion so far, the orientations of flaws with respect to the tensile stress have been ignored. There should be a distribution of flaw directions on the glass surface. Since the abrasion was carried out by rotating the rods against emery paper, most flaws should be nearly perpendicular to the line stress of the four-point bending test. If flaws of the same length are randomly distributed, the average stress on them is $2S/\pi$, or $0.636S$. However, since it is the flaw with the highest stress that propagates, flaws oriented perpendicular to the stress are preferentially selected. It is possible that orientation effects result in a somewhat lower calculated crack length than is actually present, but for the above reasons this effect should be small. Cracks may also not be perpendicular to the surface of the rod, but again because of the way the rods were abraded and perpendicular flaws selected, the effect in the calculated length should be small.

Strength distributions were calculated assuming no tip etching and the initial strength distribution given in Fig. 2. These calculated distributions are similar to the experimental ones shown in Figs. 3 and 4, except that they are displaced to somewhat lower strengths. This is the same discrepancy as shown in Fig. 1, and could again be explained as resulting from a small etching rate at the tip.

Samples aged 24 h in water showed somewhat higher strengths before etching and roughly the same relative increase in strength with etching as the unaged samples. The thickness of soda-lime glass dissolved in water at room temperature for 24 h is uncertain, but is probably considerably less than 1000 Å. Thus the strengthening by water treatment cannot be caused by decreases in the lengths of the cracks, but rather must result from a slight rounding of the tip. Therefore, water vapour apparently can diffuse to the tip and react with it, even though HF solution does not react rapidly at the tip.

Acknowledgement

This work was supported by ONR contract N00014-67-A-0117-0014-NR032-531.

References

1. F. M. ERNSBERGER, *Phys. Chem. Glasses* **10** (1969 240.
2. A. A. GRIFFITH, *Phil. Trans. Roy. Soc.* **24A** (1921) 163.
3. C. E. INGLIS, *Trans. Inst. Naval Arch.* **55** (1913) 219.
4. R. E. MOULD and R. D. SOUTHWICK, *J. Amer. Ceram. Soc.* **42** (1959) 582.
5. B. PROCTOR, *Phys. Chem. Glasses* **3** (1962) 7.
6. R. H. DOREMUS, "Glass Science" (Wiley, New York, 1973) p. 283 ff.
7. W. B. HILLIG, in "Modern Aspects of the Vitreous State", Vol. 2, (edited by J. D. Mackenzie) (Butterworths, London, 1962) p. 181 ff.
8. P. N. HOMER and B. J. CRAWFORD, *Glass Tech.* **11** (1970) 10.

Received 29 April and accepted 6 May 1974.